

Ablation of Mature miR-183 Leads to Retinal Dysfunction in Mice

Chang-Jun Zhang,^{1,2} Lue Xiang,^{1,2} Xue-Jiao Chen,^{1,2} Xiao-Yun Wang,^{1,2} Kun-Chao Wu,^{1,2} Bo-Wen Zhang,^{1,2} De-Fu Chen,^{1,2} Guang-Hui Jin,^{1,2} Hang Zhang,^{1,2} Yu-Chen Chen,^{1,2} Wei-Qin Liu,^{1,2} Meng-Lan Li,^{1,2} Yue Ma,^{1,2} and Zi-Bing Jin^{1,2}

¹Laboratory for Stem Cell & Retinal Regeneration, Institute of Stem Cell Research; Division of Ophthalmic Genetics, The Eye Hospital, Wenzhou Medical University, Wenzhou, China

²National Center for International Research in Regenerative Medicine and Neurogenetics, National Clinical Research Center for Ocular Diseases, State Key Laboratory of Ophthalmology, Optometry and Visual Science, Wenzhou, China

Correspondence: Zi-Bing Jin, Laboratory for Stem Cell & Retinal Regeneration, Institute of Stem Cell Research; Division of Ophthalmic Genetics, The Eye Hospital, Wenzhou Medical University, Wenzhou 325027, China; jinzb@mail.eye.ac.cn.

C-JZ and LX contributed equally to this work.

Received: March 25, 2019

Accepted: January 4, 2020

Published: March 16, 2020

Citation: Zhang C-J, Xiang L, Chen X-J, et al. Ablation of mature miR-183 leads to retinal dysfunction in mice. *Invest Ophthalmol Vis Sci.* 2020;61(3):12. <https://doi.org/10.1167/iovs.61.3.12>

PURPOSE. The microRNA cluster miR-183C, which includes miR-183 and two other genes, is critical for multiple sensory systems. In mouse retina, removal of this cluster results in photoreceptor defects in polarization, phototransduction, and outer segment elongation. However, the individual roles of the three components of this cluster are not clearly known. We studied the separate role of mouse miR-183 in vivo.

METHODS. miR-183 knockout mice were generated using the CRISPR/Cas9 genome-editing system. Electroretinography were carried out to investigate the changes of retinal structures and function. miR-183 was overexpressed by subretinal adeno-associated virus (AAV) injection in vivo. Rnf217, a target of miR-183 was overexpressed by cell transfection of the photoreceptor-derived cell line 661W in vitro. RNA sequencing and quantitative real-time polymerase chain reaction (qRT-PCR) were performed to compare the gene expression changes in AAV-injected mice and transfected cells.

RESULTS. The miR-183 knockout mice showed progressively attenuated electroretinogram responses. Over- or under-expression of Rnf217, a direct target of miR-183, misregulated expression of cilia-related BBSome genes. Rnf217 overexpression also led to compromised electroretinography responses in WT mice, indicating that it may contribute to functional abnormalities in miR-183 knockout mice.

CONCLUSIONS. miR-183 is essential for mouse retinal function mediated directly and indirectly through Rnf217 and cilia-related genes. Our findings provide valuable insights into the explanation and analysis of the regulatory role of the individual miR-183 in miR-183C.

Keywords: miR-183, photoreceptor, development, dysfunction, regulation

The retina is a sophisticated network of sensory and higher-order neurons that process a variety of visual information.^{1–3} Anatomically, the photoreceptors synapse directly onto bipolar cells, which subsequently synapse onto ganglion cells and ultimately conduct action potentials to the brain.⁴ Vertebrate image-forming vision relies on two types of photoreceptors, rods and cones. In mammals, rods and cones initiate two information-processing streams. Rods mediate scotopic vision at low light stimulation, but adapt or bleach with high light stimulation. Cones mediate photopic vision and are less sensitive and more resistant to bleaching.^{4–7}

Importantly, the light adaptations in the retina are regulated by different light intensities on a timescale ranging from milliseconds to hours.^{8,9} The most thoroughly studied cellular site of light–dark adaptation is the photoreceptor,^{7,9,10} in which both the light sensitivity and adaptation mechanisms have been delineated in detail.^{11,12} The sensorial neuron-specific mRNA cluster miR-183C includes miR-182, miR-183, and miR-96^{13,14} and responds to different

light conditions in mouse retinal neurons, independent of the circadian cycle.¹⁵ These microRNAs are downregulated during dark adaptation, upregulated during light adaptation, and exhibit rapid transcriptional changes. Although the importance of the photoreceptor miR-183C has been determined, the individual role of each member of this cluster is still not profoundly known.

Destruction of the miR-183C results in various retinal defects and other sensorial organ diseases.^{16,17} The most recent study using miR-183C null mice revealed that it plays a key role in the cluster for temporal regulation of the terminal differentiation of photoreceptor and hair cells.¹⁶ Moreover, a miR-183^{GT} mouse model, created using a gene trap strategy, exhibited age-dependent retinal degeneration.¹⁸ Nevertheless, separate clarification of the roles of the individual microRNAs in vivo has not been fully carried out. Therefore, we firstly generated miR-183/96 double-knockout (DKO) mice and found that complete depletion of both miR-183 and miR-96 led to defective cone nuclear polarization and progressive retinal degeneration.¹⁷ Rnf217 was further

identified as a cotarget of miR-183 and miR-96. *RNF217* codes for a 284-amino acid protein with two RING finger domains linked by an in-between-RING finger motif.¹⁹ This gene, which belongs to an ubiquitin ligase subfamily, is highly conserved across species and is highly expressed in various tissues.²⁰ However, the role of Rnf217 in the retina is currently unclear. In addition, we generated the first deletion of a single miRNA in miR-183C, miR-182 KO mice.²¹ However, it did not display apparent structural abnormalities in the retinas. To further identify its contribution to retinal function, we carried out a series of in vitro and in vivo experiments and demonstrated that the deletion of miR-182 caused mild declined electroretinography responses in mice.²²

Based on our two previous mouse models, we found that simultaneous depletion of miR-183 and miR-96 led to serious retinal defects. But miR-182 KO mice only showed slight retinal dysfunction. Moreover, miR-96 was barely expressed in cone photoreceptors.²³ Therefore, we suggested a reasonable hypothesis that miR-183 may play a dominant role in retinal functionality. To address this issue, we generated miR-183 knockout (KO) mice using the CRISPR/Cas9 genome-editing system^{24–26} and aimed to determine the effects of miR-183 on retinal maturation and function. Compared with the previously undetected abnormal phenotype in the retinal architectures of miR-182 KO mice,²¹ functionally, we observed that removing this miR-183 lead to attenuated electroretinogram (ERG) responses on different postnatal days. Furthermore, in vivo and in vitro experiments revealed that Rnf217 was regulated by miR-183 and interacted with cilia-related genes. In conclusion, we first demonstrated that miR-183 affects the maintenance of retinal function. It is essential for mouse retinal function that the appropriate expression of Rnf217 and cilia-related genes regulated by miR-183 directly and indirectly.

METHODS

Generation of miR-183 KO Mice

The miR-183 KO mice were generated in the C57BL/6 background with CRISPR/Cas9-mediated genome editing technology.^{24–26} The mouse miR-183 gene (MiRBase: MI0000225; Ensemble: ENSMUSG00000065619) is located on chromosome 6. The flanking sequence 5'-ATTCTACCAG TGCCATACAC-3' was selected as a single guide RNA to target the mouse miR-183 seed sequence. These founders were genotyped by T7E1 assay²⁷ and DNA sequence analysis (Fig. 1 and Supplementary Table S1). A mouse line carrying a 53-bp deletion (TATGGCACTGGTGTAGAATTCAGTGAACAGTCTCAGTCAAGTGAATTACCGAAG) around the miR-183 seed sequence was selected and bred for this project.

Targeted Deep Sequencing of Candidate Off-Target Sites

We used Cas-OFFinder²⁸ for off-target identification in the *Mus musculus* (mm10) reference genome, and the top 10 most likely potential off-target sites were predicted. The PCR fragments of the on-target and off-target sites were amplified using the primers (Supplementary Table S2) in the KO and control mouse retinal samples and analyzed by targeted next-generation sequencing. The PCR products were gel purified using Monarch DNA Gel Extraction Kit (New England Biolabs, Ipswich, MA) and quantified using

Qubit 3.0 Fluorometer (Life Technologies, Carlsbad, CA). Next, the DNA Library was established using TruSeq DNA Library Prep Kits (Illumina, San Diego, CA) following the manufacturer's protocol. Then, paired-end sequencing of DNA Library was subjected to the HiSeq X Ten platform (Illumina). Finally, by analysis in comparison with the control group, potential off-target effects were verified in multiple KO mouse retinal tissues.

Animal Care and Use

The animal resource center of Wenzhou Medical University handled and maintained all experimental animals, where they were housed under a 12-hour light–dark cycle and given a standard chow diet. Animal care followed the guidelines formulated by the Association for Research in Vision and Ophthalmology (ARVO). Experiments and procedures involving animals were permitted by the Animal Care and Use Committees of Wenzhou Medical University. Mice of both sexes were used in this study.

ERG

The miR-183 KO mice and age-matched wild-type (WT) controls were paired for Micron IV focal ERGs (fERGs). Micron IV fERGs were carried out following the instruction manual (Phoenix Research Labs, Pleasanton, CA). Mice were dark adapted for 12 hours and anesthetized intraperitoneally with a mixture of ketamine (80 mg/kg) and xylazine (16 mg/kg). The pupils were dilated with 0.5% tropicamide for 10 minutes, and corneas were anesthetized with 0.5% phenylephrine. A drop of Gen Teal lubricant eye gel (Novartis, East Hanover, NJ) was applied on the surface of the cornea to keep the cornea moist, and gold wire loop electrodes were placed over the corneas. Mice were placed on a 37°C warming pad to maintain the body temperature. Then, fERGs were measured with red light illumination as previously described.¹⁷ The gradient stimulus intensities used for the photopic fERGs were provided at light levels 0.7, 1.4, 2.1, 3.0, and 3.3 log (cd·s/m²). Each light level corresponded to a stimulus frequency of 20, 20, 10, 5, and 5 sweeps, respectively. The delay between sweeps was 0.7, 0.7, 10.0, 20.0, and 20.0 seconds, respectively. The gradient stimulus intensities used for the scotopic fERG were provided at light levels –1.7, –0.7, 0.3, 2.1, and 3.0 log (cd·s /m²). Each light level corresponded to a stimulus frequency 20, 20, 10, and 5 sweeps. The delay between sweeps was 0.7, 0.7, 0.7, 10.0, and 20.0 seconds, respectively.

RNA Isolation and Quantitative RT-PCR (qRT-PCR)

Both retinas of each mouse were dissected, and the total RNA was extracted using TRIzol reagent (Life Technologies) and RNeasy Mini Kit (Qiagen, Duesseldorf, Germany). The extracted RNA was quantified on a NanoDropND-1000 spectrophotometer (Thermo Fisher Scientific, Grand Island, NY). For analysis of miRNA levels, cDNA was prepared using AMV Reverse Transcriptase (Takara Bio, Kusatsu, Japan) and a stem-loop RT primer. qRT-PCR was carried out using a TaqMan PCR kit and a 7500 Sequence Detection System (Applied Biosystems, Carlsbad, CA). For mRNAs, total RNA was reverse transcribed into cDNA with M-MLV reverse transcriptase (Promega, Madison, WI) and random primers (Promega). qRT-PCR was performed using the Applied Biosystems Step One System using a standard protocol

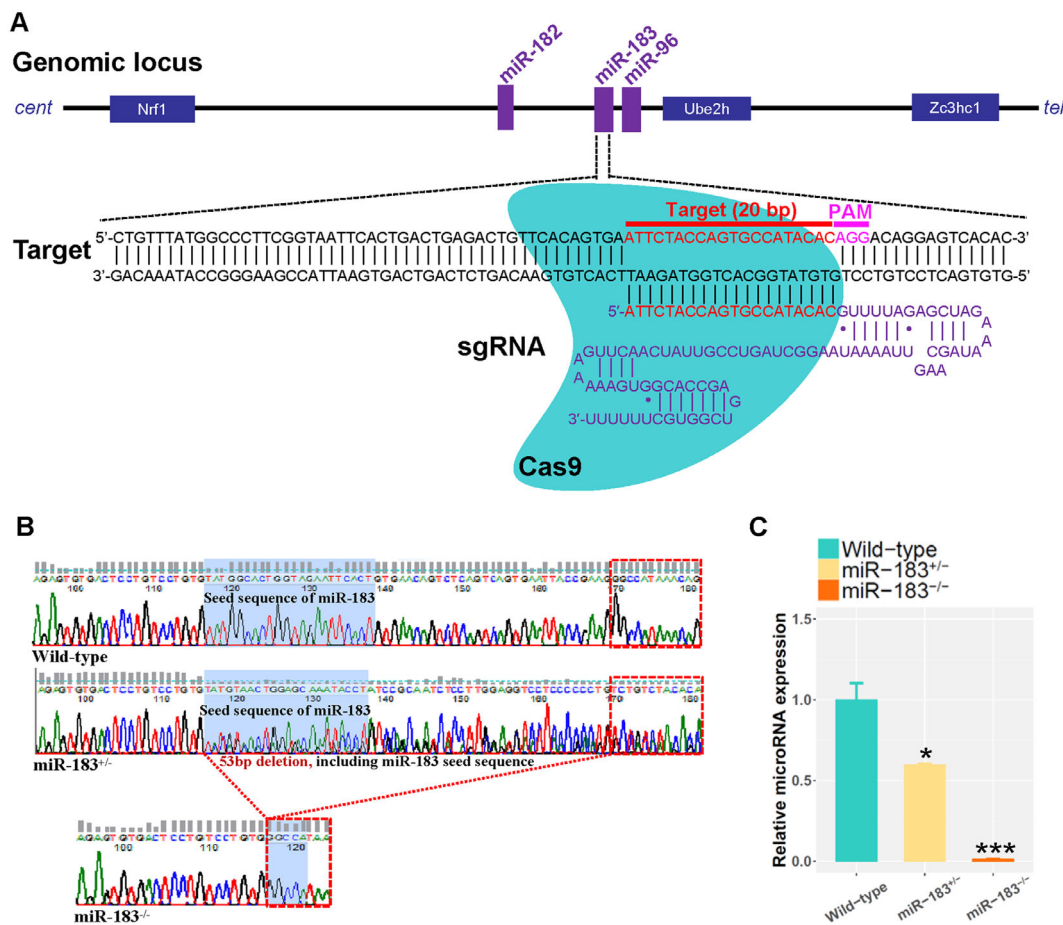


FIGURE 1. Complete deletion of miR-183 by CRISPR/Cas9-mediated genome engineering technology in the mouse germ line. (A) Location of mouse miR-183 in the genomic organization and map of the Cas9 protein bound to the single guide RNAs. The Cas9 nuclease from *S. pyogenes* (in *aquamarine*) targets the 22-nucleotide sequences in miR-183 (red) by a single guide RNA consisting of a 22-nt guide sequence (red) and a scaffold (purple). The guide sequence pairs with the DNA target (red bar on the top strand), directly upstream of a requisite 5'-NGG adjacent motif (PAM; pink). tel, telomeric; cent, centromeric. (B) Genotyping strategy for the WT mice and mutants (miR-183^{-/-}) by DNA sequencing. The sequencing samples of the pair-wise sequence comparison between WT, heterozygous (miR-183^{+/-}), and miR-183^{-/-} mice are shown. WT DNA was used as a negative control for sequencing in parallel. Blue shade, the seed sequence of miR-183. Red dotted line, the 53-bp deletion including the miR-183 seed sequence of miR-183^{-/-} mice. (C) qRT-PCR analysis ($n = 3$) of miR-183 expression at P30 in the retinas of the WT, homozygous (miR-183^{-/-}), and heterozygous (miR-183^{+/-}) mice, respectively. Relative expression levels of microRNAs were normalized to the level of U6. * $P < 0.05$, *** $P < 0.001$ between the miR-183^{-/-} mice and littermates, Student *t*-test.

with cDNA, SYBR Green PCR master mix (Roche Applied Science, Indianapolis, IN), and specific primers (Supplementary Table S3).²⁹

Western Blot Analysis

Total protein was extracted from tissues or cells using lysis buffer containing protease inhibitors. The extracted proteins were quantified with the Pierce BCA Protein Assay Kit (Thermo Fisher Scientific), separated by 12% sodium dodecyl sulfate polyacrylamide gel electrophoresis and electrotransferred onto a nitrocellulose blotting membrane (PALL Corporation, Port Washington, NY). The membranes were blocked for 1 h in 5% skim milk in 1 × Tris-buffered saline Tween and incubated overnight with primary antibodies at 4°C. Last, the membranes were incubated with secondary antibodies at room temperature for 1 hour. Fluorophore-conjugated antibodies were detected using the Odyssey Imager (LI-COR Biosciences Inc., Lincoln, NE). The

primary antibodies used were mouse anti-Rnf217 (1:500, Santa Cruz Biotechnology, Santa Cruz, CA) and mouse anti-β-actin (1:2000, KangChen Bio-tech, Shanghai, China). The secondary antibodies were IRDye 680-conjugated goat anti-rabbit (Abcam, Cambridge, Cambridgeshire, UK) and IRDye 800CW-conjugated goat anti-mouse (Abcam).

RNA-Sequencing Analyses

Total RNA was extracted from WT retinas according to the instruction manual of the Trizol Reagent (Life Technologies) at different developmental times (E13.5 to P45). The cDNA library was constructed using an Illumina HiSeq 2500 sequencing platform. Gene expression levels were estimated using fragment per kilobase of exon per million fragments mapped values by the Cufflinks software (Supplementary Table S4). The differentially expressed genes in WT retinas were processed by gene ontology analyses.

Plasmid Construction, Transfection, and Cell Culture

To overexpress Rnf217 in *in vitro* experiments, plasmids (primer sets in Supplementary Table S5) were constructed and transfected into cells of the photoreceptor-derived cell line 661W (Department of Cell Biology, University of Oklahoma Health Sciences Center, Oklahoma City, OK) using a transfection reagent (Lipofectamine 2000; Invitrogen, Carlsbad, CA). Another group of 661W cells treated with PBS served as the control group. The 661W cells were cultured in Dulbecco's modified Eagle's medium (Life Technologies) containing 10% fetal bovine serum (Gibco, Waltham, MA; Thermo Fisher Scientific) and 100 U/mL penicillin-streptomycin (Thermo Fisher Scientific).³⁰

Adeno-Associated Virus (AAV) 2/8-Mediated miR-183 and Rnf217 Overexpression

The packaged plasmids of AAV2/8-mediated miR-183 and Rnf217 (Supplementary Table S6) overexpression were constructed as described previously.¹⁷ The target sequence of AAV2/8-mmu-miR-183 was cloned into the NheI and HindIII sites of a GV412 vector containing CMV bGlobin-EGFP-MCS. The target sequence of AAV2/8-mmu-Rnf217 was cloned into the BamHI/BamHI sites of a GV467 vector containing CMV-bGlobin-MCS-EGFP-3Flag. An AAV2/8-mediated empty vector containing CMV-bGlobin-EGFP was used as the negative control. The inserted sequence was generated by qRT-PCR using the primers listed in Supplementary Table S6. The titers of AAV2/8-mmu-miR-183, AAV2/8-mmu-Rnf217, and AAV2/8-CMV-bGlobin-eGFP were 5.13×10^{12} TU/mL, 2.5×10^{12} TU/mL, and 3.76×10^{12} TU/mL, respectively.

AAV Injections

Four-week-old C57BL/6J WT mice were anesthetized by ketamine and xylazine (as described in the ERG protocol elsewhere in this article) at P30. After dilation with 0.5% tropicamide for 10 minutes, the eyes were gently protruded and subsequently covered with 2% hydroxypropyl methylcellulose in PBS, allowing surgery to be performed under an operating microscope. A small incision was created away from the lens near the sclera with a sharp 30-G hypodermic needle. Then, a total of 1 μ L (1×10^{12} TU/mL) of AAV-mmu-Rnf217, AAV-mmu-miR-183 for the right eye and control vector for the left eye were injected slowly into the subretinal space between the retina and RPE using a blunt 5- μ L Hamilton syringe held in a micromanipulator. The mark of a successful injection was the presence of a retinal detachment.

Statistical Analyses

All results are presented as the means \pm SEM, and statistical significance was assessed using a two-tailed Student *t*-test. The results were visualized using R project as previously described.³¹ **P* < 0.05, ***P* < 0.01, and ****P* < 0.001 between the KO and WT groups or experimental and control groups.

RESULTS

Precise Deletion of the miR-183 Seed Sequence in Mice

The three components of miR-183C, that is, miR-182, miR-183, and miR-96, have highly similar seed regions and extensive overlap in their predicted targets.¹³ The particularly interesting characteristics of this genome organization prompted us to understand the individual roles of the components of this cluster in mice. Structurally, miR-183C spans more than 15 kB with several potent exons scattered between the three microRNA members. Therefore, to avoid interfering with any potential epigenetic motifs, we needed to perform precise editing of the microRNAs in this region. CRISPR/Cas9-mediated genome engineering technology²⁴⁻²⁶ allowed for the design of miR-183-specific single guide RNAs to generate a KO mouse model, termed miR-183^{-/-} mice (Fig. 1A). The positive founders that carried a 53-bp deletion (including the miR-183 seed sequence) were identified by a T7E1 assay²⁷ and DNA sequencing analysis. Then, their offspring were genotyped by DNA sequencing after reproducing several generations (Fig. 1B). To verify and exclude potential off-target effects, we selected the top 10 candidate off-target sites²⁸ and assayed by targeted next-generation sequencing. Through sequence analysis in comparison with the control group, no off-target sites were identified in multiple KO mouse retinal tissues. qRT-PCR targeting the seed sequence of miR-183 validated the absence of this microRNA expression in the homozygous (miR-183^{-/-}) mice (Fig. 1C). Accordingly, its expression was decreased to 59.6% in the heterozygous (miR-183^{+/-}) mice (Fig. 1C). Our KO model was demonstrated to successfully and precisely knock out the miR-183 sequence without impacting other regions of the genome in mice.

Deletion of Mature miR-183 Leads to Progressively Attenuated ERG Responses

Data obtained in previous studies using the DKO mouse model suggested that the photopic ERG responses were abolished as early as P30.¹⁷ In our study, the lack of the miR-183 seed sequence in mice had a mild influence on the ERG responses (Fig. 2). At P30, the earliest evaluation time point, the miR-183 KO mice displayed significantly lower b-wave amplitudes than WT mice in the photopic ERG responses, but not flat waves (decreased to 39.4% at the highest stimulus intensity; Fig. 2A, right). Interestingly, unlike the observation in DKO mice,¹⁷ the scotopic ERG b-wave in miR-183^{-/-} mice had a lower amplitude than its WT counterpart (decreased to 61.3% at the highest stimulus intensity; Fig. 2A, left). In general, the scotopic rather than the photopic ERG amplitudes declined progressively at the next two inspected time points, P90 and P180 (Fig. 2B-D). These two time points showed a much more obvious decrease in the scotopic amplitudes from P30 (with b-wave amplitudes in miR-183^{-/-} mice decreasing from 61.3% to 46.5% at the highest stimulus intensity) than those in the photopic ones (decreasing from 39.4% to 32.9%; Fig. 2B, D). Taken together, the ERG experiments demonstrated that precise removal of miR-183 resulted in a mild and progressive deterioration on retinal functions.

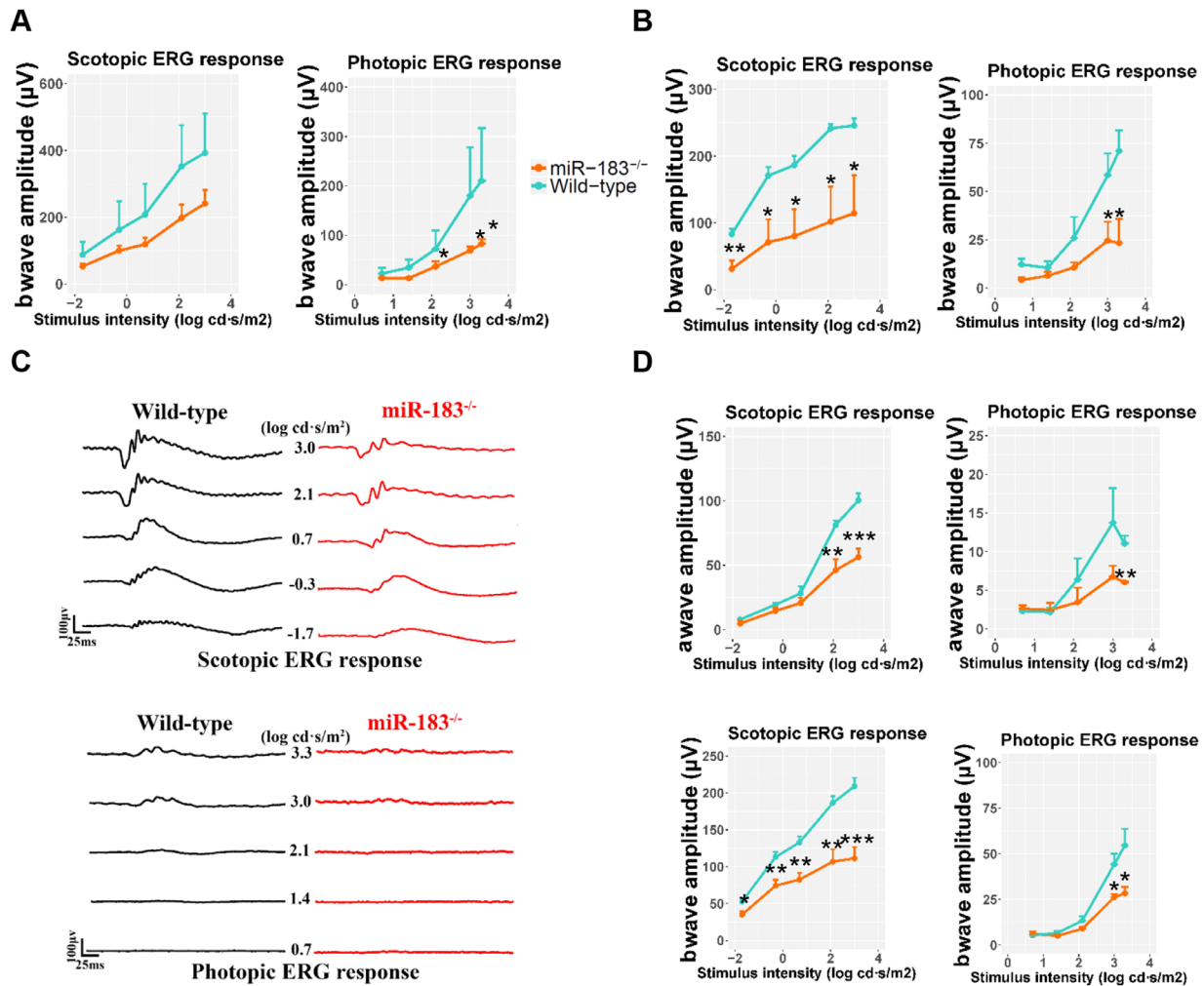


FIGURE 2. Deletion of the miR-183 gene resulted in progressive defects in ERG responses in the mouse retina. ERG recordings were obtained from adult mice at P30, P90, and P180 at different stimulus intensities. (A) Quantitative measurements of scotopic, reflecting mostly rod activity (*left* in A, B, and D), and photopic, reflecting mostly cone activity (*right* in A, B, D). There were some significant differences in either a-wave or b-wave amplitude at P30 (A), P90 (B), and P180 (C, D) between miR-183^{-/-} and age-matched WT mice stimulated with light of the indicated intensities. WT mice: $n = 4, 5,$ and 4 for P30, P90, and P180, respectively; miR-183^{-/-} mice: $n = 7, 3,$ and 5 for P30, P90, and P180, respectively. (C) Representative scotopic and photopic ERG recording curves of P180 mice. * $P < 0.05,$ ** $P < 0.01,$ *** $P < 0.001,$ Student t -test.

Rnf217 Modulates the Expression of Cilia-Related Genes in Photoreceptors

Our previous study found that Rnf217, which is regulated by miR-183, was a cotarget of miR-183 and miR-96.¹⁷ In addition, RNF2, a ring finger protein, have been reported to interact with some cilia-related BBS proteins (BBS1, BBS2, BBS4, and BBS7) in the progress of protein degradation.³² As with RNF2, RNF217 was also a ring finger protein,¹⁹ which can also degrade target proteins by ubiquitination.²⁰ Therefore, we proposed that Rnf217 might regulate the expression of some cilia-related BBSome genes in the retina. To test this hypothesis, we first analyzed our in-house normal data at different developmental timepoints and found that Rnf217 expression decreased across development (Fig. 3A). Simultaneously, the expression of the miR-183 cluster¹⁷ and cilia-related BBSome genes in WT mouse retinas increased across development (Fig. 3A).

We then confirmed Rnf217 as a target of miR-183 by Western blotting at P30 and P180 (Fig. 3D). Consistently, in

vitro experiments verified that overexpression of Rnf217 in 661W cells repressed expression of some of the cilia-related BBSome genes (Figs. 3B, C). Moreover, overexpression of miR-183 in the retinas led to the downregulation of Rnf217 and misregulation of cilia-related BBSome genes (Fig. 3E). Previous studies showed that cilia-related BBSome genes (e.g., Bbs1 to Bbs10) are associated with primary cilia formation and photoreceptor functionalization in the eye.^{33–35} And aberrant expression of cilia-related BBSome genes could lead to a ciliopathy, Bardet-Biedl syndrome.^{36,37} Bardet-Biedl syndrome is an autosomal-recessive disease characterized by defects in multiple systems, including retinal dystrophy, hypogonadism, renal abnormalities, obesity, mental retardation, and dystrophic extremities.^{37,38} Furthermore, abnormal expression of BBSome genes are able to cause retinal disorganized ERG response.^{39–42} Therefore, it may be the cause of the defective ERG in miR-183 KO mice. Taken together, our results provided evidence showing that Rnf217, as a direct target of miR-183, affects the normal expression of cilia-related BBSome genes.

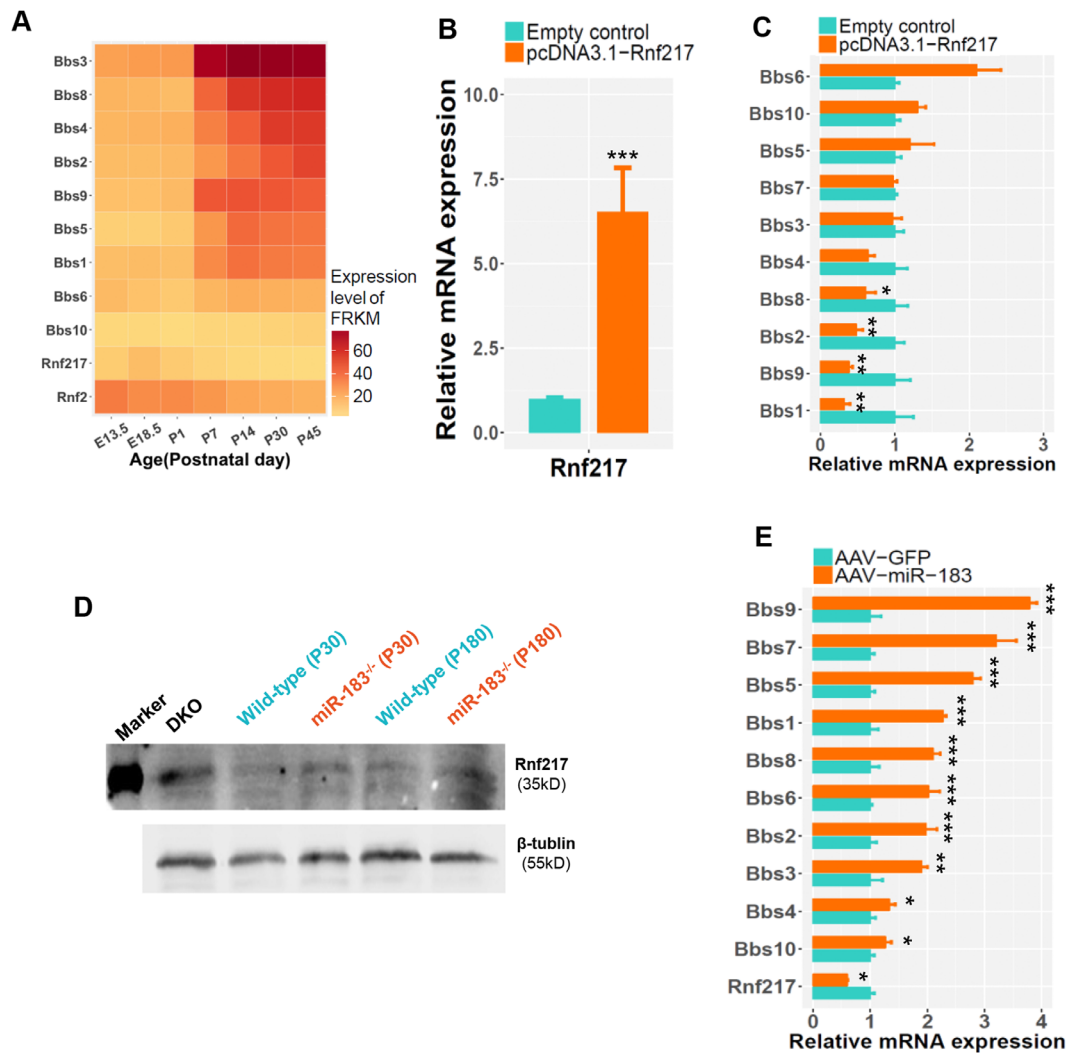


FIGURE 3. Rnf217 is regulated by miR-183 and negatively regulates BBSome genes in photoreceptors. (A) The relative expression of Rnf2, Rnf217, and BBSome genes based on in-house RNA sequencing data on a log₂ scale indicated that Rnf217 expression was inhibited in parallel with the accumulation of BBSome genes in the developing mouse retina from P0 onward. (B and C) Overexpression of Rnf217 (B) in 661W cells leads to the downregulation of most BBSome genes (including Bbs1, 2, 8, and 9) as determined by quantitative RT-PCR (qRT-PCR) assay (C). (D) The RNF217 level was higher in miR-183^{-/-} mouse retinas (brown) than in the retinas of WT littermates (*aquamarine*) as shown by Western blot analysis at P30 and P180. The DKO mouse retina served as a positive control, and tubulin served as a loading control (*bottom*). The first band is a marker standard, glyceraldehyde-3-phosphate dehydrogenase. (E) Overexpression of miR-183 in WT retinas transfected with miR-183-overexpressing AAV vectors resulted in downregulation of Rnf217 and upregulation of some BBSome genes. **P* < 0.05; ***P* < 0.01; ****P* < 0.001.

Overexpression of Rnf217 is Detrimental to Mouse ERG Responses

Across development, the expression levels of Rnf2 decreased gradually with different developmental stages in mouse retinas (Fig. 3A). Separately, Rnf217 was downregulated after birth, indicating that it is unnecessary in the postnatal stages (Fig. 3A). However, the specific role of Rnf217 in the retina has not been studied. To verify whether or not Rnf217 overexpression in miR-183 KO mice was the cause of the attenuated ERG responses, we ectopically expressed this gene in WT mice. Overexpression was carried out at P30, and ERG and RNA analysis were performed on retinas at P50 (Fig. 4A). By using an AAV-mediated subretinal injection, we successfully introduced this gene (Fig. 4B) into retinas with a 47-fold enhancement in expression as measured by qRT-

PCR (Fig. 4C). As expected, compared with the waves in the control virus-injected eyes, there were significant decreases in scotopic a-wave and b-wave amplitudes in the treated eyes at the highest stimulus intensity (scotopic b-wave amplitude decreased to 68.9%; a-wave amplitude decreased to 62.6%; Fig. 4D). However, there were no significant changes in the photopic a-wave and b-wave amplitudes (data not shown). These results indicated that the direct regulation of Rnf217 expression by miR-183 supported the functionalities of both rods and cones. Overexpression of Rnf217 may be detrimental to miR-183 KO mouse ERG responses.

DISCUSSION

Retinitis pigmentosa is a dominant cause of inherited blindness that results from a remarkably progressive retinal

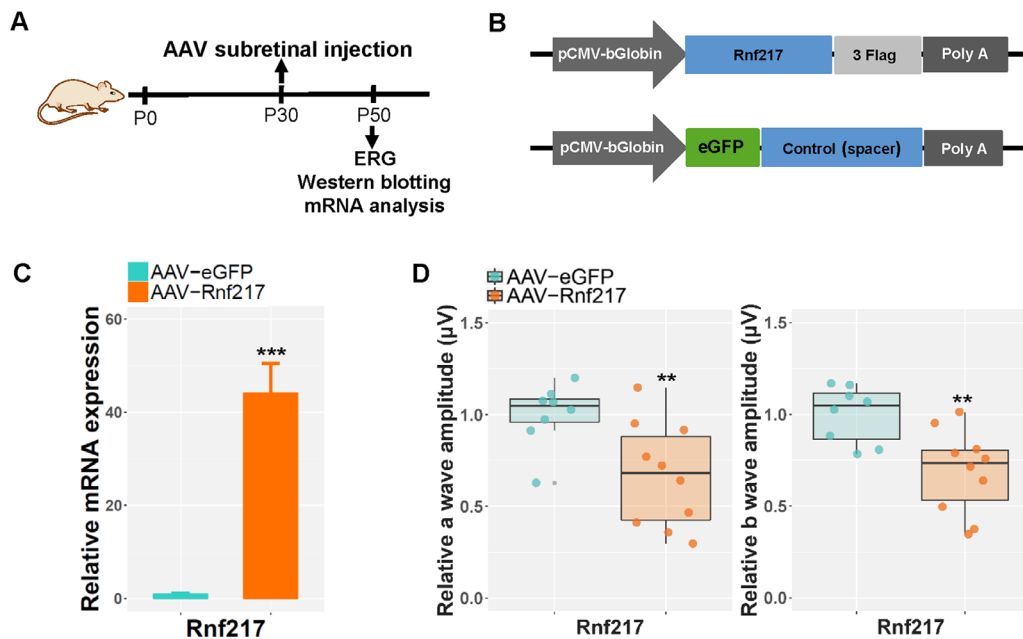


FIGURE 4. Overexpression of Rnf217 is detrimental to the mouse retina. **(A)** Schematic representation of the experiments showing important time points. **(B)** AAV-mediated Rnf217 overexpression and control expression (OS, left eye) cassettes were driven by the pCMV-bGlobin promoter. Spacer sequences were inserted downstream of eGFP into the AAV vectors. **(C)** Rnf217 expression in AAV-Rnf217-injected retinas was much greater than in the AAV-eGFP-injected WT retinas (OS) as analyzed by qRT-PCR ($n = 3$). **(D)** Significantly attenuated scotopic ERG responses appeared in the eyes injected with AAV-Rnf217 compared with the control eyes. AAV-Rnf217 subretinal injection, $n = 10$; AAV-eGFP ($n = 10$). * $P < 0.05$; ** $P < 0.01$; *** $P < 0.001$; Student *t*-test.

degeneration.⁴³ There is evidence that gene mutations, including microRNA genes, are causally associated with this and other forms of inherited retinal degeneration.^{44–51} Interestingly, inactivation of miR-183C causes various defects in the visual, auditory, vestibular, and olfactory systems during the terminal differentiation stage.^{16–18,21,23,52–57} By precisely editing the miR-183 seed sequence in mice, we revealed that this microRNA is indispensable for the maintenance of retinal function. Removing the seed sequence of miR-183 directly or indirectly led to downstream mRNA misregulation, which may finally contribute to the compromised ERG responses. This finding extended our understanding of the typical roles of the individual microRNAs in the miR-183C cluster.

So far, the role of most abundant miR-183C or its individual member (miR-182 or miR-96) in sensory nervous system has been well studied in last decade.^{16–18,21,22,23,52–57} Previous studies demonstrated the complete deletion of mouse miR-183C led to dysmaturity of sensory receptor precursors, sequential delay of outer segment elongation, and malposition of cone photoreceptors with serious and broad vision loss.¹⁶ Similarly, our previous miR-183/96 DKO mice also exhibited severe defective cone maturation and progressive photoreceptor degeneration with compromised ERG responses. Unexpectedly, the ablation of single mouse miR-182 did not give rise to any apparent defects in retinal architecture, but resulted in mildly decreased ERG responses. These inconsistent discoveries aroused our interests in exploring the individual role of 183 and 96 on retina. miR-96 was expressed at a very low level in mouse retina compared with miR-183 and miR-182¹³ and was abundant in hair cells.⁵⁶

Based on these previous observations,¹³ we reasoned that miR-183 may be a dominant factor for retinal development. However, our miR-183 KO model showed mild progressive retinal dysfunction. This observation prompted us to hypothesize that, instead of miR-183, other factors within the KO region of the DKO mice may be the hidden contributors to the retinal degeneration.¹⁷ Thereinto, the inhibition of miR-96 led to eye malformations as well as defects in cranial cartilage development in zebrafish.⁵⁸ Xu et al.¹³ reported that the miR-183 cluster is located in an intron that envelopes three potential exon genes and spans more than 15 kb on mouse Chr6qA3.3. Therefore, we developed a second hypothesis that the predicted exons, located upstream and downstream of the miR-183 cluster, may play important regulatory roles in forming and maintaining retinal functionality and organization. In contrast, noncoding RNA has the potential to interact with microRNA.⁵⁹ Therefore, this suggests a third hypothesis, that is, that regulatory noncoding RNA within the region that indirectly influences retinal structure and function. Further studies are required to test and verify the three hypotheses as suggested.

Photoreceptor functions are regulated by various transcriptional factors.^{60,61} Cilia-related genes play an important role in primary cilia formation and photoreceptor functionalization in the eye.^{33–35} Moreover, aberrant expression of cilia-related genes could cause some abnormalities in ERG response.^{39–42} We found significant misregulation of cilia-related gene expression in miR-183^{-/-} mice, suggesting that it could lead to defects in retinal function. However, the Rnf217 protein is a putative E3 ubiquitin protein ligase, which degrades target proteins by ubiquitination.²⁰ Whether Rnf217 accounts for the ubiquitination of the cilia-related genes needs further investigation. In addition, depletion of

BBS8 perturbs olfactory function, and some patients with Bardet-Biedl syndrome exhibit hearing loss,^{62,63} suggesting that miR-183-mediated regulation of Rnf217 may exist in other sensory neurons as well.

Precise deletion of miR-183 resulted in the upregulation of Rnf217 and misregulation of cilia-related genes in mice. Overexpression of Rnf217 in WT mice resulted in perturbed ERG responses, which were also observed in miR-183 KO mice. These findings are consistent with the known misregulation of mouse cilia-related genes that cause retinal dysfunction.^{62,63} Thus, the miR-183- and Rnf217-mediated gene networks may serve as a fundamental component in the maintenance of normal mouse ERG responses.

Taken together, our findings demonstrate that miR-183 is necessary for retinal functionality in mice. ERG responses are primarily affected by disturbances in miR-183-mediated mis-expression. Proper Rnf217 and cilia-related gene expression, regulated directly and indirectly by miR-183 across development, is indispensable for mouse retinal function. Our findings demonstrate that miR-183-mediated gene regulation is essential for retinal functionality.

Acknowledgments

The authors thank the Specific Pathogen Free (SPF) animal facility at Wenzhou Medical University for supporting this project.

Supported by the National Key R&D Program of China (2017YFA0105300, 2017YFB0403702 [Z-BJ]), National Natural Science Foundation of China (81970838 [Z-BJ], 81870690 [X-JC], 81800857 [LX]), Zhejiang Provincial Natural Science Foundation of China (LD18H120001LD [Z-BJ]). The authors alone are responsible for the content and writing of the paper.

Disclosure: **C.-J. Zhang**, None; **L. Xiang**, None; **X.-J. Chen**, None; **X.-Y. Wang**, None; **K.-C. Wu**, None; **B.-W. Zhang**, None; **D.-F. Chen**, None; **G.-H. Jin**, None; **H. Zhang**, None; **Y.-C. Chen**, None; **W.-Q. Liu**, None; **M.-L. Li**, None; **Y. Ma**, None; **Z.-B. Jin**, None

References

1. Van Essen DC, Anderson CH, Felleman DJ. Information processing in the primate visual system: an integrated systems perspective. *Science*. 1992;255:419–423.
2. Kanwisher N, Wojciulik E. Visual attention: insights from brain imaging. *Nat Rev Neurosci*. 2000;1:91–100.
3. Masland RH. The fundamental plan of the retina. *Nat Neurosci*. 2001;4:877–886.
4. Provencio I, Rollag MD, Castrucci AM. Photoreceptive net in the mammalian retina. This mesh of cells may explain how some blind mice can still tell day from night. *Nature*. 2002;415:493.
5. Hattar S, Lucas RJ, Mrosovsky N, et al. Melanopsin and rod-cone photoreceptive systems account for all major accessory visual functions in mice. *Nature*. 2003;424:76–81.
6. Fu Y, Liao HW, Do MT, Yau KW. Non-image-forming ocular photoreception in vertebrates. *Curr Opin Neurobiol*. 2005;15:415–422.
7. Fu Y, Yau KW. Phototransduction in mouse rods and cones. *Pflugers Arch*. 2007;454:805–819.
8. Wässle H. Parallel processing in the mammalian retina. *Nat Rev Neurosci*. 2004;5:747–757.
9. Morshedjian A, Fain GL. Light adaptation and the evolution of vertebrate photoreceptors. *J Physiol*. 2017;595:4947–4960.
10. Paul KN, Saafir TB, Tosini G. The role of retinal photoreceptors in the regulation of circadian rhythms. *Rev Endocr Metab Disord*. 2009;10:271–278.
11. Provencio I, Foster RG. Circadian rhythms in mice can be regulated by photoreceptors with cone-like characteristics. *Brain Res*. 1995;694:183–190.
12. Pugh EN, Jr., Nikonov S, Lamb TD. Molecular mechanisms of vertebrate photoreceptor light adaptation. *Curr Opin Neurobiol*. 1999;9:410–418.
13. Xu S, Witmer PD, Lumayag S, Kovacs B, Valle D. MicroRNA (miRNA) transcriptome of mouse retina and identification of a sensory organ-specific miRNA cluster. *J Biol Chem*. 2007;282:25053–25066.
14. Peng C, Li L, Zhang MD, et al. miR-183 cluster scales mechanical pain sensitivity by regulating basal and neuropathic pain genes. *Science*. 2017;356:1168–1171.
15. Krol J, Busskamp V, Markiewicz I, et al. Characterizing light-regulated retinal microRNAs reveals rapid turnover as a common property of neuronal microRNAs. *Cell*. 2010;141:618–631.
16. Fan J, Jia L, Li Y, et al. Maturation arrest in early postnatal sensory receptors by deletion of the miR-183/96/182 cluster in mouse. *Proc Natl Acad Sci USA*. 2017;114:E4271–E4280.
17. Xiang L, Chen XJ, Wu KC, et al. miR-183/96 plays a pivotal regulatory role in mouse photoreceptor maturation and maintenance. *Proc Natl Acad Sci USA*. 2017;114:6376–6381.
18. Lumayag S, Haldin CE, Corbett NJ, et al. Inactivation of the microRNA-183/96/182 cluster results in syndromic retinal degeneration. *Proc Natl Acad Sci USA*. 2013;110:E507–516.
19. Fontanari Krause LM, Japp AS, Krause A, et al. Identification and characterization of OSTL (RNF217) encoding a RING-IBR-RING protein adjacent to a translocation breakpoint involving ETV6 in childhood ALL. *Sci Rep*. 2014;4:6565.
20. Ho SR, Lee YJ, Lin WC. Regulation of RNF144A E3 Ubiquitin Ligase Activity by Self-association through Its Transmembrane Domain. *J Biol Chem*. 2015;290:23026–23038.
21. Jin ZB, Hirokawa G, Gui L, et al. Targeted deletion of miR-182, an abundant retinal microRNA. *Mol Vis*. 2009;15:523–533.
22. Wu KC, Chen XJ, Jin GH, et al. Deletion of miR-182 leads to retinal dysfunction in mice. *Invest Ophthalmol Vis Sci*. 2019;60:1265–1274.
23. Busskamp V, Krol J, Nelidova D, et al. miRNAs 182 and 183 are necessary to maintain adult cone photoreceptor outer segments and visual function. *Neuron*. 2014;83:586–600.
24. Li D, Qiu Z, Shao Y, et al. Heritable gene targeting in the mouse and rat using a CRISPR-Cas system. *Nat Biotechnol*. 2013;31:681–683.
25. Cong L, Zhang F. Genome engineering using CRISPR-Cas9 system. *Methods Mol Biol*. 2015;1239:197–217.
26. Zhang YH, Wu LZ, Liang HL, et al. Pulmonary surfactant synthesis in miRNA-26a-1/miRNA-26a-2 double knockout mice generated using the CRISPR/Cas9 system. *Am J Transl Res*. 2017;9:355–365.
27. Shen B, Zhang W, Zhang J, et al. Efficient genome modification by CRISPR-Cas9 nickase with minimal off-target effects. *Nat Methods*. 2014;11:399–402.
28. Bae S, Park J, Kim JS. Cas-OFFinder: a fast and versatile algorithm that searches for potential off-target sites of Cas9 RNA-guided endonucleases. *Bioinformatics*. 2014;30:1473–1475.
29. Jin ZB, Huang XF, Lv JN, et al. SLC7A14 linked to autosomal recessive retinitis pigmentosa. *Nat Commun*. 2014;5:3517.
30. Gao ML, Wu KC, Deng WL, et al. Toll-like receptor 3 activation initiates photoreceptor cell death in vivo and in vitro. *Invest Ophthalmol Vis Sci*. 2017;58:801–811.

31. Paradis E, Claude J, Strimmer K. APE: analyses of phylogenetics and evolution in R language. *Bioinformatics*. 2004;20:289–290.
32. Gascue C, Tan PL, Cardenas-Rodriguez M, et al. Direct role of Bardet-Biedl syndrome proteins in transcriptional regulation. *J Cell Sci*. 2012;125:362–375.
33. Jin H, White SR, Shida T, et al. The conserved Bardet-Biedl syndrome proteins assemble a coat that traffics membrane proteins to cilia. *Cell*. 2010;141:1208–1219.
34. Pretorius PR, Baye LM, Nishimura DY, et al. Identification and functional analysis of the vision-specific BBS3 (ARL6) long isoform. *PLoS Genet*. 2010;6:e1000884.
35. Pretorius PR, Aldahmesh MA, Alkuraya FS, Sheffield VC, Slusarski DC. Functional analysis of BBS3 A89V that results in non-syndromic retinal degeneration. *Human Mol Genet*. 2011;20:1625–1632.
36. Forsythe E, Beales PL. Bardet-Biedl syndrome. *Eur J Hum Genet*. 2013;21:8–13.
37. Forsythe E, Beales PL. Bardet-Biedl syndrome. *Eur J Hum Genet*. 2013;21:8–13.
38. Tsang SH, Aycinena ARP, Sharma T. Ciliopathy: Bardet-Biedl syndrome. *Adv Exp Med Biol*. 1085:171–174.
39. Cox GF, Hansen RM, Quinn N, Fulton AB. Retinal function in carriers of Bardet-Biedl syndrome. *Arch Ophthalmol*. 2003;121:804–810.
40. Kim LS, Fishman GA, Seiple WH, Szlyk JP, Stone EM. Retinal dysfunction in carriers of Bardet-Biedl syndrome. *Ophthalmic Genet*. 2007;28:163–168.
41. Abd-El-Barr MM, Sykoudis K, Andrabi S, et al. Impaired photoreceptor protein transport and synaptic transmission in a mouse model of Bardet-Biedl syndrome. *Vision Res*. 2007;47:3394–3407.
42. Daniels AB, Sandberg MA, Chen J, Weigel-DiFranco C, Fielding Hejtmancic J, Berson EL. Genotype-phenotype correlations in Bardet-Biedl syndrome. *Arch Ophthalmol*. 2012;130:901–907.
43. Hartong DT, Berson EL, Dryja TP. Retinitis pigmentosa. *Lancet*. 2006;368:1795–1809.
44. Loscher CJ, Hokamp K, Kenna PF, et al. Altered retinal microRNA expression profile in a mouse model of retinitis pigmentosa. *Genome Biol*. 2007;8:R248.
45. Loscher CJ, Hokamp K, Wilson JH, et al. A common microRNA signature in mouse models of retinal degeneration. *Exp Eye Res*. 2008;87:529–534.
46. Dalgard CL, Gonzalez M, deNiro JE, O'Brien JM. Differential microRNA-34a expression and tumor suppressor function in retinoblastoma cells. *Invest Ophthalmol Vis Sci*. 2009;50:4542–4551.
47. Sanuki R, Onishi A, Koike C, et al. miR-124a is required for hippocampal axogenesis and retinal cone survival through Lhx2 suppression. *Nat Neurosci*. 2011;14:1125–1134.
48. Ran X, Cai WJ, Huang XF, et al. 'RetinoGenetics': a comprehensive mutation database for genes related to inherited retinal degeneration. *Database (Oxford)*. 2014;2014.
49. Huang XF, Wu J, Lv JN, Zhang X, Jin ZB. Identification of false-negative mutations missed by next-generation sequencing in retinitis pigmentosa patients: a complementary approach to clinical genetic diagnostic testing. *Genet Med*. 2015;17:307–311.
50. Huang XF, Huang ZQ, Fang XL, Chen ZJ, Cheng W, Jin ZB. Retinal miRNAs variations in a large cohort of inherited retinal disease. *Ophthalmic Genet*. 2017;39:175–179.
51. Huang XF, Huang F, Wu KC, et al. Genotype-phenotype correlation and mutation spectrum in a large cohort of patients with inherited retinal dystrophy revealed by next-generation sequencing. *Genet Med*. 2015;17:271–278.
52. Damiani D, Alexander JJ, O'Rourke JR, et al. Dicer inactivation leads to progressive functional and structural degeneration of the mouse retina. *J Neurosci*. 2008;28:4878–4887.
53. Lewis MA, Quint E, Glazier AM, et al. An ENU-induced mutation of miR-96 associated with progressive hearing loss in mice. *Nat Genet*. 2009;41:614–618.
54. Li H, Kloosterman W, Fekete DM. MicroRNA-183 family members regulate sensorineural fates in the inner ear. *J Neurosci*. 2010;30:3254–3263.
55. Zhu Q, Sun W, Okano K, et al. Sponge transgenic mouse model reveals important roles for the microRNA-183 (miR-183)/96/182 cluster in postmitotic photoreceptors of the retina. *J Biol Chem*. 2011;286:31749–31760.
56. Kuhn S, Johnson SL, Furness DN, et al. miR-96 regulates the progression of differentiation in mammalian cochlear inner and outer hair cells. *Proc Natl Acad Sci USA*. 2011;108:2355–2360.
57. Ubhi K, Rockenstein E, Kragh C, et al. Widespread microRNA dysregulation in multiple system atrophy - disease-related alteration in miR-96. *Eur J Neurosci*. 2014;39:1026–1041.
58. Gessert S, Bugner V, Tecza A, Pinker M, Kuhl M. FMR1/FXR1 and the miRNA pathway are required for eye and neural crest development. *Dev Biol*. 2010;341:222–235.
59. Krol J, Krol I, Alvarez CP, et al. A network comprising short and long noncoding RNAs and RNA helicase controls mouse retina architecture. *Nat Commun*. 2015;6:7305.
60. Hennig AK, Peng GH, Chen S. Regulation of photoreceptor gene expression by Crx-associated transcription factor network. *Brain Res*. 2008;1192:114–133.
61. Peng GH, Chen S. Active opsin loci adopt intrachromosomal loops that depend on the photoreceptor transcription factor network. *Proc Natl Acad Sci USA*. 2011;108:17821–17826.
62. Beales PL, Warner AM, Hitman GA, Thakker R, Flinter FA. Bardet-Biedl syndrome: a molecular and phenotypic study of 18 families. *J Med Genet*. 1997;34:92–98.
63. Tadenev AL, Kulaga HM, May-Simera HL, Kelley MW, Katsanis N, Reed RR. Loss of Bardet-Biedl syndrome protein-8 (BBS8) perturbs olfactory function, protein localization, and axon targeting. *Proc Natl Acad Sci USA*. 2011;108:10320–10325.